Draft version August 31, 2025
Typeset using LaTeX **twocolumn** style in AASTeX7

The Impact of an AGN Continuum on PAH Features in a Simulated Galaxy

Grant P. Donnelly [1], Desika Narayanan [2], Paul Torrey [3] and J.D.T. Smith [1]

[1] *Ritter Astrophysical Research Center, University of Toledo, Toledo, OH 43606, USA*
[2] *Department of Astronomy, University of Florida, 211 Bryant Space Sciences Center, Gainesville, FL 32611 USA*
[3] *Department of Astronomy, University of Virginia, 530 McCormick Road, Charlottesville, VA 22903, USA*

ABSTRACT

Galaxies hosting an active galactic nucleus (AGN) show diminished power and altered spectral feature ratios from polycyclic aromatic hydrocarbons (PAHs) compared with normal star-forming galaxies. Proposed mechanisms for this include AGN-driven PAH grain processing and continuum dilution: the observational implications of the bright AGN continuum and heating of the interstellar medium (ISM). These potentially competing factors are difficult to disentangle observationally. In this work, we address this issue theoretically using a hydrodynamically simulated galaxy from `AREPO` and the post-processing radiative transfer code `POWDERDAY`, focusing on the effects of continuum dilution. We find that independent of grain processing, but not mutually exclusive with it, the continuum effects are capable of obfuscating PAH emission even when it is in fact present. Additionally, the AGN impacts observed PAH band ratios.

Keywords: Polycyclic aromatic hydrocarbons (1280), Galaxies (573), AGN host galaxies (2017), Astronomical simulations (1857), Interstellar dust (836)

1. INTRODUCTION

The mid-infrared (MIR) spectral emission features arising from interstellar polycyclic aromatic hydrocarbons (PAHs) are altered, diminished, or even absent in galaxies where an active galactic nucleus (AGN) is present (e.g. Aitken & Roche 1985; Moorwood 1986; Smith et al. 2007; O'Dowd et al. 2009; Diamond-Stanic & Rieke 2010), compared to the PAH-dominated global spectra of normal star-formng galaxies where variations are relatively muted. Less affected by extinction than optical/UV diagnostics, PAH emission is an increasingly common indicator for the star-formation rate (e.g. Peeters et al. 2004; Shipley et al. 2016; Lai et al. 2020) and is a promising probe for conditions in the interstellar medium (ISM) such as the molecular gas content (Chown et al. 2025). However, the changes to PAH spectra when an AGN is present make these uses difficult to interpret for those galaxies.

It is common to ascribe these different PAH spectra to an influence of the AGN on PAH grains themselves; the hard radiation emitted by an AGN could destroy PAH grains, leading to an overall reduction in PAH emission (Aitken & Roche 1985; Voit 1992). For AGN-hosting galaxies in which PAH emission is observed, short-to-long wavelength PAH ratios are suppressed (e.g. Smith et al. 2007; O'Dowd et al. 2009; Sales et al. 2010; García-Bernete et al. 2022), possibly indicating that an AGN preferentially destroys the smaller (and perhaps more brittle) PAH grains, which tend to emit more power at shorter wavelengths (Draine et al. 2021). Thus, an AGN may play a significant role in the evolution of the dust grain size distribution (GSD) within a galaxy.

Emssion from the nuclear environment extrinsically affects observed PAH spectra too. The spectral energy distribution (SED) of an AGN holds significant power at infrared wavelengths due to re-emission by a surrounding dusty torus structure (Pier & Krolik 1992; Nenkova et al. 2008a,b) and by heating the broader extra-nuclear ISM . This manifests in the MIR as a continuum that can dilute PAH features and make them difficult or impossible to observe, even if present. Further, since individual PAH features have different widths and relative strengths, the sloped AGN continuum could differentially affect PAH band ratios as it dilutes the PAH features. The apparent lack of PAH emission reported by early, necessarily large-aperture, MIR studies of local AGN-hosts was likely influenced by this dilution effect. With JWST or Spitzer, continuum dilution effects are minimal in the extended regions of nearby resolved galaxies, but it will still hinder the study of PAHs in the nucleus where any impact by the AGN on PAHs would be the most significant. On the other hand, the observed SEDs of unresolved, distant AGN-hosts and quasars include a blend of AGN and host galaxy components by definition. This is a source of uncertainty for current studies of PAHs at high redshift, and will be a source of uncertainty for future far-infrared facilities like PRIMA as they use PAHs to track the accumulation of metals throughout cosmic time.

Corresponding author: Grant P. Donnelly

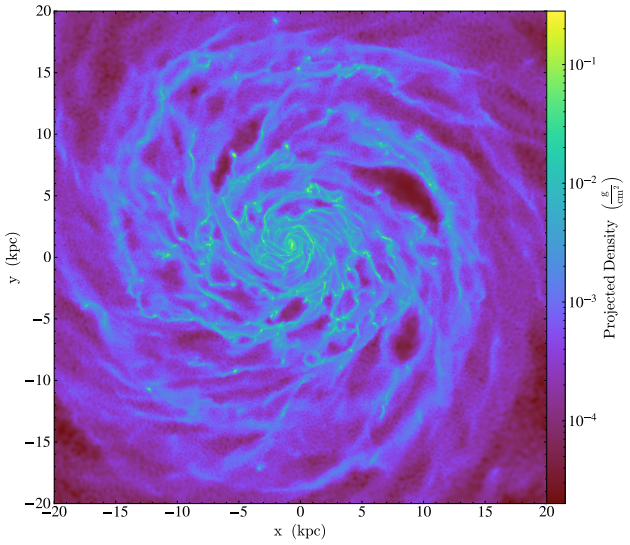

Figure 1. Projected gas density for the AREPO+SMUGGLE simulated galaxy. The galaxy is a Milky Way analog. Here, it is 2 Gyr old.

Observationally, it is difficult to separate the competing effects of continuum dilution and possible AGN-driven PAH grain destruction. Several studies have modeled the impact of PAH-AGN continuum dilution (e.g. Lutz et al. 1998; Xie & Ho 2022), but so far each of these have been forced to treat the AGN and host galaxy (including PAH) SED components as separable and independent. Thus, investigating this problem using simulated galaxies instead may be helpful. Recent radiative transfer codes such as POWDERDAY (Narayanan et al. 2021), through the theoretical PAH emission models of Draine et al. (2021), have enabled the study of simulated PAH spectra that are sensitive to changes in the radiation field hardness and intensity, as well as the grain size and ionization state distributions. The purpose of this work is to use POWDERDAY to, for the first time, include an AGN as a radiation component for PAHs in a simulated galaxy, and to determine how continuum dilution affects the PAH emission in the resulting galaxy SED in the context of self-consistent radiative transfer. This is a necessary step for future studies to properly interpret the SEDs of simulated galaxies that model AGN-driven PAH processing.

2. SIMULATED AGN-HOST GALAXY SPECTRA

Our goal is to produce simulated MIR spectra of an AGN-host, so we must first produce a simulated galaxy. In this section, we describe how we generated such a galaxy and modeled the radiative transfer in it.

2.1. *Galaxy Formation and Evolution*

In general, we follow the framework outlined by Narayanan et al. (2023) (N23), which uses AREPO (Springel 2010; Weinberger et al. 2020) for the hydrodynamical simulation and the SMUGGLE module (Marinacci et al. 2019) for the galaxy formation and evolution processes: the evolution in the star-formation rate, dust production and destruction, and evolution in the dust GSD. The initial conditions for our galaxy are similar to the idealized Milky Way analog from N23, which followed Hopkins et al. (2011). The galaxy is allowed to evolve until it has reached a steady-state, after 2 Gyr (see Figure 1). In order to most easily interpret the observed effects of the AGN on the output SED, and for simplicity, the AGN is only introduced during the post-processesing radiative transfer simulation (see §2.2). It does not impact the galaxy evolution. In this way, we have produced a scenario analogous to a AGN that recently turned on.

2.2. *Radiative Transfer Simulations*

Since we are focusing on the PAH spectra, we employ the POWDERDAY (Narayanan et al. 2021) code to facilitate the radiative transfer. POWDERDAY is built on top of HYPERION (Robitaille 2011). Using the PAH emission models from Draine et al. (2021), which are sensitive to the intensity and hardness of the interstellar radiation field (ISRF), as well as the distribution of PAH sizes and ionization states, POWDERDAY can self-consistently model the PAH emssion within our simulated galaxy. In order to prevent infinities due to unresolved distances between PAHs and star-forming regions, we set $\log U = 0$, where U is the dust heating parameter relative to the ISRF within the solar neighborhood (see Draine et al. 2021). By definition, $\log U = 0$ is typical in the ISM, and the PAH spectrum is insensitive to this value over a few orders of magniftude, not until $\log U \gtrsim 3$. Further, we disable the treatment of gas-phase emission lines since we are only interested in the dust emission here.

2.3. *POWDERDAY with an AGN*

POWDERDAY supports AGN, or black holes generally, as luminous point sources with some SED shape in the radiative transfer. We implement an AGN in our model by placing a black hole in the exact center of the simulated galaxy, with a mass equal to that of Sgr A*, $M_{\rm BH} = 4.3 \times 10^6\,{\rm M}_\odot$ (GRAVITY Collaboration et al. 2022). It is important to note here that AGN-driven grain processing is not modelled in this simulation, in order to isolate the observational effects on PAHs from the AGN radiation. For the black hole SED, we use the models from Hopkins et al. (2007) (H07, see the blue line in Figure 2), which critically includes the infrared component from hot dust torus surrounding the nucleus. The MIR spectrum of an AGN often includes broad features centered ≈10 and 18μm from silicate-rich dust grains in the torus (Nenkova et al. 2008a,b), and these features can appear in either absorption or emission, depending on the viewing angle of the AGN geometry. These increase the complexity of accurately fitting

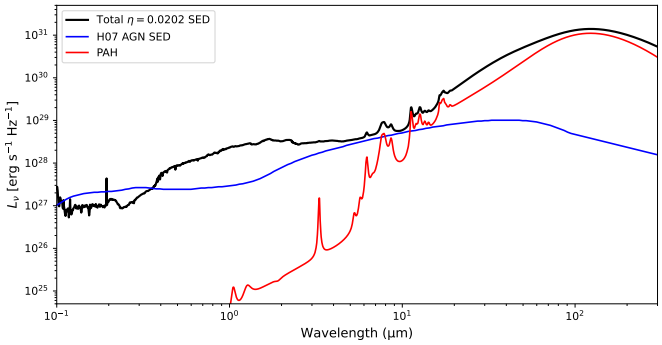

Figure 2. Example decomposed global SED for the simulated galaxy with a low-luminosity AGN ($\eta = 0.0202$). The black line is the total SED including all luminous sources, including the AGN, after the radiative transfer, and the red line shows the PAH-only spectrum after radiative transfer. The blue line is the unattenuated Hopkins et al. (2007) template AGN SED scaled to the present AGN luminosity. Note that even at this low η, the PAHs have been noticably diluted.

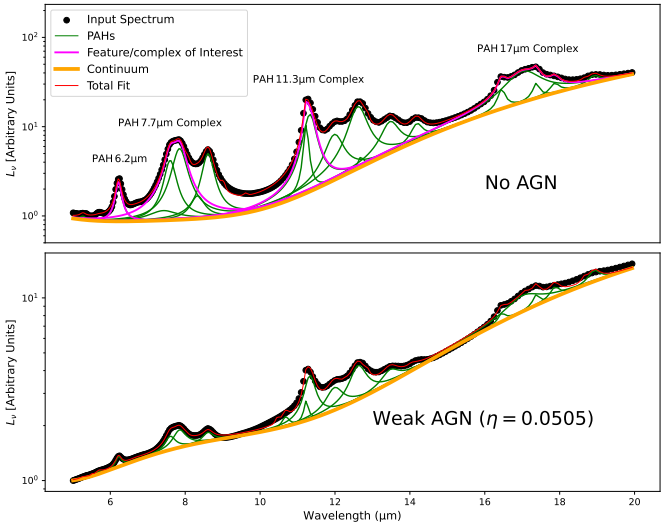

Figure 3. Examples of `PAHFIT` spectral decompositions. In both panels, the black dots are luminosity densities of `POWDERDAY` SEDs, the orange line is the fitted continuum (starlight and dust-emitted modified blackbodies), and the green profiles (Drude profiles) represent individual PAH features. The red line is the total fitted model. In the top panel, magenta lines highlight the features of interest in this work, and they show the extent of PAH complexes. The top panel shows the AGN-free galaxy, and the bottom panel shows the spectrum from a relatively weak ($\eta = 0.0505$) AGN.

PAH features, and they would complicate the interpretation of how the AGN continuum impacts the visibility of PAH emission within our experiment. The H07 template provides the advantage of a relatively featureless continuum, without built-in silicate features.

The AGN SED is then scaled such that its integral is equal to the input black hole luminosity. A useful benchmark for AGN luminosity is the Eddington luminosity, which is set by $M_{\rm BH}$,

$$L_{\rm Edd} = 1.25 \times 10^{38}\,{\rm erg\,s^{-1}} (M_{\rm BH}/{\rm M}_\odot)\,. \quad (1)$$

For Sgr A*, $L_{\rm Edd} = 5.4 \times 10^{44}\,{\rm erg\,s^{-1}}$. In this work, we scale the AGN luminosity in terms of the Eddington efficiency, η, where

$$\eta = \frac{L_{\rm AGN}}{L_{\rm Edd}}\,. \quad (2)$$

Typical values for η among nearby AGN-hosts range from $\approx 10^{-3}$ to ≈ 1 (Gupta et al. 2025). Though short-timescale AGN variability can be modeled by `POWDERDAY`, we simulate an unvarying AGN here. We ran 100 `POWDERDAY` simulations on the MW-analog galaxy between $10^{-2} \leqslant \eta \leqslant 1$.

2.4. *SED Extraction and Fitting*

We extract a galaxy-wide SED for each `POWDERDAY` run using the built-in functionality from `HYPERION`, see an example in Figure 2. Since this work is concerned with the observational implications of an AGN on how PAH emission is quantified, we use the `PAHFIT` (Smith et al. 2007) spectral decomposition tool that has been commonly used for Spitzer/IRS and JWST spectra. `PAHFIT` simultaneously fits models for individual PAH features as Drude profiles and continuum sources as modified blackbodies. Figure 3 gives two examples of simulated spectra fit with `PAHFIT`. Each green Drude profile represents a certain PAH vibrational mode, but it is also common to refer to PAH feature complexes that consist of multiple modes, as we do here, but we refer to these two terms (feature/complex) interchangeably. In Figure 3, we highlight the main PAH features and complexes that we analyze in this work. In order to directly compare the how PAH features are affected between different `POWDERDAY` simulations with different AGN luminosities, we consider the PAH equivalent width (EW), which we compute with

$${\rm EW} = \frac{F_{\rm PAH} \times 10^{20}}{\nu F_\nu^{\rm cont}}\,, \quad (3)$$

where $F_{\rm PAH}$ is the `PAHFIT` surface flux of the feature in ${\rm W\,m^{-2}\,sr^{-1}}$, ν is the central frequency of the feature in Hz, and $F_\nu^{\rm cont}$ is the value of the fitted `PAHFIT` continuum at the central wavelength of the feature in ${\rm MJy\,sr^{-1}}$.

3. RESULTS

In Figure 4, we show the 2—20 μm spectra from several of the `POWDERDAY` radiative transfer simulations with different values of η. The spectrum from the simulation with no AGN ($\eta = 0$) presents PAH features typical of a normal star-forming galaxy, and the simulation with the

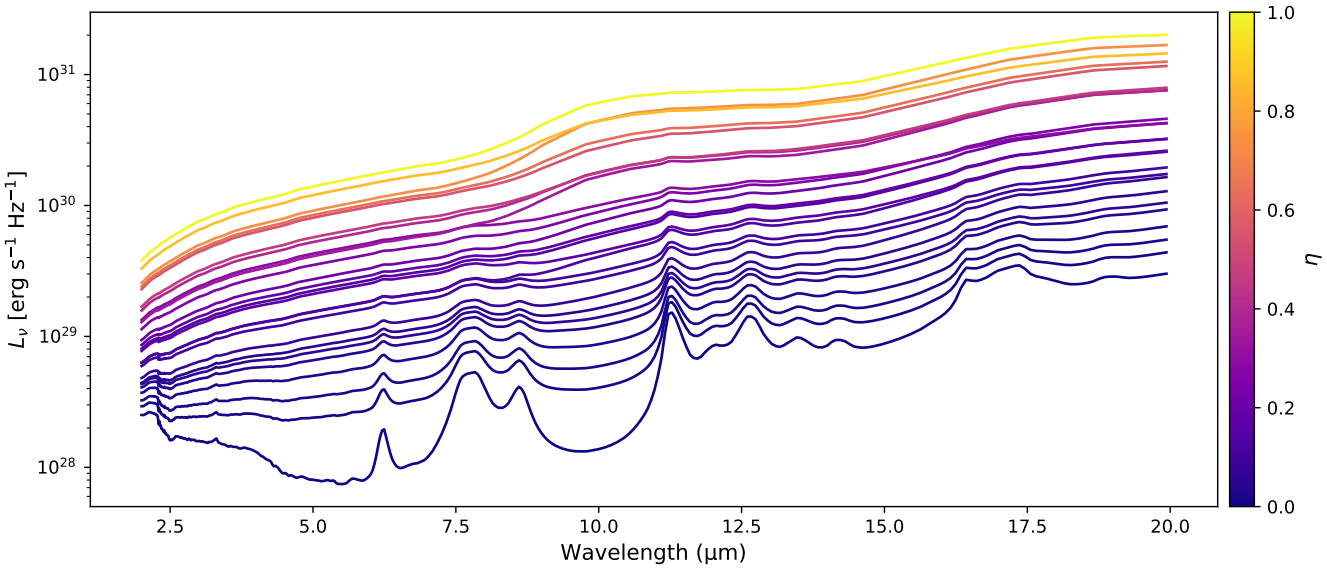

Figure 4. A subset of the MIR spectra extracted from our simulated galaxy with different AGN luminosity scale factors η. Different colors represent different `POWDERDAY` simulations with different values of η, and in this shown sample the values of η are logarithmically spaced. At low η, PAH spectra are prominent, but apparently disappear as the AGN luminsity increases. At high values of η, silicate emission features appear from hot dust in the ISM.

most luminous AGN in our set ($\eta = 1$), no PAH features are visible. This is despite the fact that the $\eta = 1$ galaxy has nearly just as much PAH emission as the galaxy with no AGN, since the morphologies, star-formation rates, and dust abundances are identical. At the intermediate values of η, the PAH features progressively disappear as the contribution from the AGN dilutes them until a nearly smooth continuum is all that remains.

The only noticable features in the spectra with the highest η are broad bumps at $\approx$10 μm and $\approx$18 μm corresponding to emission from hot silicate grains. Such features are common in the spectra of AGN due to the presence and relative desnity of silicate grains at high temperatures in the torus structures that surround AGN, and may instead be seen in absorption depending on the viewing angle. However, the Hopkins et al. (2007) AGN templates are agnostic of silicate features (i.e. Figure 2), meaning that these emssion bumps are coming from hot silicate grains in the ISM. Since they overlap with PAH features, the presence of the silicate emission bumps affect how the progressively brighter AGN alters PAH EW and band ratios, as described below.

The different PAH features are affected differently by the increasing AGN continuum. In Figure 4, this is apparent by-eye as even for high values of η when all other PAH features have become indeterminable, the PAH 11.3 μm feature is still visible. Factors that determine how much an individual PAH feature is affected by continuum dilution include: the shape of the PAH feature, the slope of the AGN continuum, and the presence of silicate features. We quantified how the sum of these effects vary with η using `PAHFIT`, and the results are shown in Figure 5. The top panel, which tracks the equivalent width of four major PAH features, demonstrates what is seen by-eye in Figure 4: as the AGN luminosity increases, the prominence of *all* PAH features suffer. However, they are each affected at different rates.

4. DISCUSSION

In Figures 4 and 5, we show how an AGN with different luminosities can alter the observed PAH spectrum of a Milky Way-like galaxy, even though the PAH abundance and grain properties are unchanged in each case. Due to the effect of continuum dilution, PAH features become too difficult to distinguish and accurately quantify. Thus, derived PAH abundances from spectra would be systematically underestimated in unresolved AGN-hosts, and in the nucelar regions of nearby AGN-hosts. We also showed that PAH band ratios are affected by the AGN continuum. Additionally, the presence of emission features that arise from AGN-heated silicate grains in the broader ISM are an example of how MIR spectra (and thus PAHs) are affected even off-nucleus. Though these results are not mutually exclusive with the picture that an AGN destroys PAH grains, and perhaps preferentially the smaller PAHs, they demsonstrate that AGN continuum dilution is an important competing factor to consider.

As part of an effort to determine whether intense star-formation or AGN are the dominant power source in ultraluminous infrared galaxies (ULIRGs), Genzel et al. (1998) proposed a diagram that uses PAH EW to separate these two groups, on the grounds that values are smaller for galaxies with an AGN. In principle, this method is naturally agnostic of the reason for the smaller

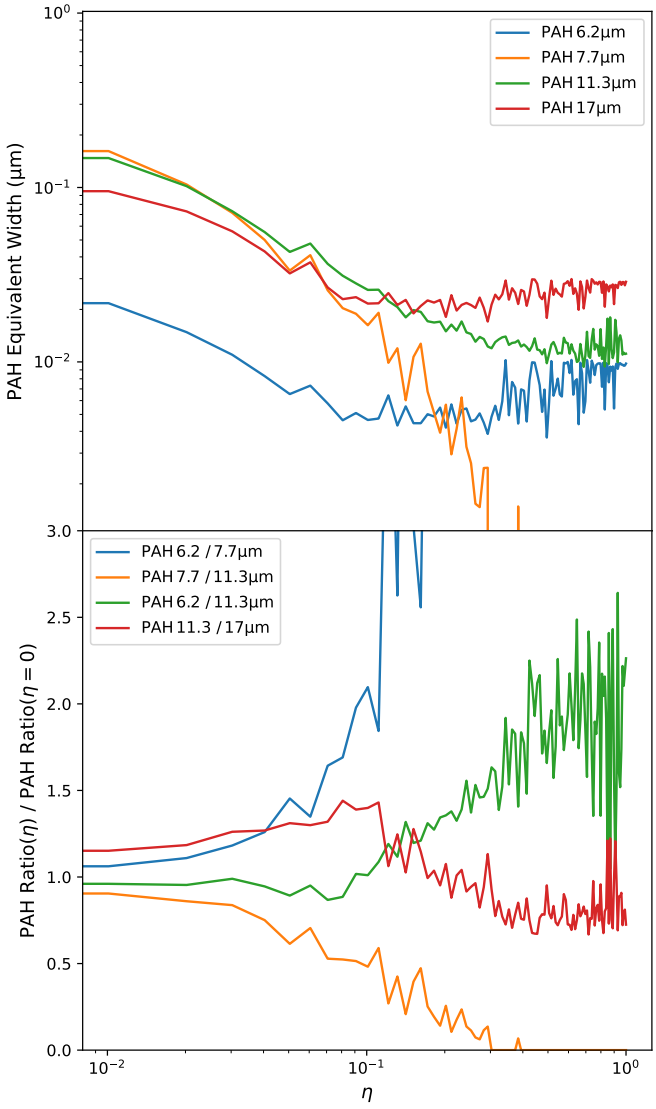

Figure 5. The results from the PAHFIT fits for each POWDERDAY simulation. Top: the measured PAH equivalent width (EW) as a function of the AGN luminosity scale factor η for four major PAH bands. In each case, the EW decreases with increasing AGN luminosity due to continuum dilution. Bottom: how four short-to-long wavelength PAH band ratios change with increasing η, each relative to the value of that ratio for the AGN-free galaxy.

PAH EWs, and numerous successive works have used it for this purpose (e.g. Laurent et al. 2000; Tran et al. 2001; Armus et al. 2007; Rich et al. 2023). Our results are consistent with the picture that the PAH EW diagnostic is practical even if there are no alterations to PAH properties made by an AGN. In dusty, star-forming, high metallicity galaxies where the MIR continuum is not dominated by light from evolved stars, the only source capable of producing the temperatures required for a strong continuum at these wavelengths is an AGN.

There are a few important notes regarding specific interpretations of our results. First, the particular way that the AGN continuum across a range of luminosities dilutes PAH features and alters their ratios is sensitive to the choice of AGN SED shape, as well as factors that determine the independent PAH spectrum like the GSD, ionization, and stellar radiation field. Thus, a different choice of AGN SED or a non-Milky Way analog simulated galaxy would have changed the rates at which the PAH spectrum is altered. For example, an AGN SED that includes silicate features in absorption or emission stands to dramatically change the way that PAHs overlapping with these features are measured. However, these would not change our main conclusion that increasingly bright AGN continuua dilute PAH features and change their ratios.

Second, our results are somewhat sensitive to our particular choice of using PAHFIT as the spectral decomposition tool. Other tools exist, such as CAFE (Marshall et al. 2007; Diaz-Santos et al. 2025) or the method described in Xie et al. (2018). Since these model the PAHs and continuua differently, each may perform better or worse at quantifying the true PAH flux for a low-luminosity AGN. However, it is unlikely that the results would be much different as the PAH features become indistinguishable from the continuum, as is shown in the fitting model-independent Figure 4.

Finally, POWDERDAY is a post-processing radiative transfer code. Since the AGN was only included at this stage, and not in the galaxy evolution simulation, it has no impact on other galaxy properties that would impact the MIR spectra, such as the star-formation rate history that influences the excitation of the PAHs and therefore their spectral feature strengths. Thus, the scenario outlined in this work is applicable first and foremost to a normal star-forming galaxy that has very recently had an AGN turn on. However, it is entirely possible to produce a wide range of different scenarios to that are testable with POWDERDAY post-processing, including initial conditions that simulate a galaxy that has been subject to AGN feedback. This may be the subjet of future work.

5. CONCLUSIONS

In the observed MIR spectra of galaxies, those with an AGN tend to exhibit PAH bands with different ratios and that are overall fainter compared to normal star-forming galaxies. In this work, we used the POWDERDAY ratiative transfer code to test what impact the inclusion of an AGN has on the PAH spectrum of a simulated galaxy, without any grain-processing physics driven by the AGN. These are our main conclusions:

1. Through a combination of continuum dilution and ISM heating, the AGN is capable of apparently di-

minishing or obfuscating PAH emission from observed spectra.

2. Likewise, the AGN continuum is capable of altering PAH band ratios, complicating interpretations of AGN-driven grain processing in observed galaxies.

3. The use of the PAH equivalent width as an AGN diagnostic is practical for galaxies not dominated by starlight from evolved populations.

ACKNOWLEDGEMENTS

This work originated from a project of the Summer Program in Astrophysics 2025 held at the University of Virginia, and funded by the Center for Global Inquiry and Innovation, the National Science Foundation (Grant 2452494), the National Radio Astronomy Observatory (NRAO), the Kavli Foundation and the Heising-Simons Foundation.

REFERENCES

Aitken, D. K., & Roche, P. F. 1985, MNRAS, 213, 777, doi: 10.1093/mnras/213.4.777

Armus, L., Charmandaris, V., Bernard-Salas, J., et al. 2007, ApJ, 656, 148, doi: 10.1086/510107

Chown, R., Leroy, A. K., Sandstrom, K., et al. 2025, ApJ, 983, 64, doi: 10.3847/1538-4357/adbd40

Diamond-Stanic, A. M., & Rieke, G. H. 2010, ApJ, 724, 140, doi: 10.1088/0004-637X/724/1/140

Diaz-Santos, T., Lai, T. S. Y., Finnerty, L., et al. 2025, CAFE: Continuum And Feature Extraction tool, Astrophysics Source Code Library, record ascl:2501.001

Draine, B. T., Li, A., Hensley, B. S., et al. 2021, ApJ, 917, 3, doi: 10.3847/1538-4357/abff51

García-Bernete, I., Rigopoulou, D., Alonso-Herrero, A., et al. 2022, MNRAS, 509, 4256, doi: 10.1093/mnras/stab3127

Genzel, R., Lutz, D., Sturm, E., et al. 1998, ApJ, 498, 579, doi: 10.1086/305576

GRAVITY Collaboration, Abuter, R., Aimar, N., et al. 2022, A&A, 657, L12, doi: 10.1051/0004-6361/202142465

Gupta, K. K., Ricci, C., Tortosa, A., et al. 2025, arXiv e-prints, arXiv:2507.12541, doi: 10.48550/arXiv.2507.12541

Hopkins, P. F., Quataert, E., & Murray, N. 2011, MNRAS, 417, 950, doi: 10.1111/j.1365-2966.2011.19306.x

Hopkins, P. F., Richards, G. T., & Hernquist, L. 2007, ApJ, 654, 731, doi: 10.1086/509629

Lai, T. S. Y., Smith, J. D. T., Baba, S., Spoon, H. W. W., & Imanishi, M. 2020, ApJ, 905, 55, doi: 10.3847/1538-4357/abc002

Laurent, O., Mirabel, I. F., Charmandaris, V., et al. 2000, A&A, 359, 887, doi: 10.48550/arXiv.astro-ph/0005376

Lutz, D., Spoon, H. W. W., Rigopoulou, D., Moorwood, A. F. M., & Genzel, R. 1998, ApJL, 505, L103, doi: 10.1086/311614

Marinacci, F., Sales, L. V., Vogelsberger, M., Torrey, P., & Springel, V. 2019, MNRAS, 489, 4233, doi: 10.1093/mnras/stz2391

Marshall, J. A., Herter, T. L., Armus, L., et al. 2007, ApJ, 670, 129, doi: 10.1086/521588

Moorwood, A. F. M. 1986, A&A, 166, 4

Narayanan, D., Turk, M. J., Robitaille, T., et al. 2021, ApJS, 252, 12, doi: 10.3847/1538-4365/abc487

Narayanan, D., Smith, J. D. T., Hensley, B. S., et al. 2023, ApJ, 951, 100, doi: 10.3847/1538-4357/accf8d

Nenkova, M., Sirocky, M. M., Ivezić, Ž., & Elitzur, M. 2008a, ApJ, 685, 147, doi: 10.1086/590482

Nenkova, M., Sirocky, M. M., Nikutta, R., Ivezić, Ž., & Elitzur, M. 2008b, ApJ, 685, 160, doi: 10.1086/590483

O'Dowd, M. J., Schiminovich, D., Johnson, B. D., et al. 2009, ApJ, 705, 885, doi: 10.1088/0004-637X/705/1/885

Peeters, E., Spoon, H. W. W., & Tielens, A. G. G. M. 2004, ApJ, 613, 986, doi: 10.1086/423237

Pier, E. A., & Krolik, J. H. 1992, ApJ, 401, 99, doi: 10.1086/172042

Rich, J., Aalto, S., Evans, A. S., et al. 2023, ApJL, 944, L50, doi: 10.3847/2041-8213/acb2b8

Robitaille, T. P. 2011, A&A, 536, A79, doi: 10.1051/0004-6361/201117150

Sales, D. A., Pastoriza, M. G., & Riffel, R. 2010, ApJ, 725, 605, doi: 10.1088/0004-637X/725/1/605

Shipley, H. V., Papovich, C., Rieke, G. H., Brown, M. J. I., & Moustakas, J. 2016, ApJ, 818, 60, doi: 10.3847/0004-637X/818/1/60

Smith, J. D. T., Draine, B. T., Dale, D. A., et al. 2007, ApJ, 656, 770, doi: 10.1086/510549

Springel, V. 2010, MNRAS, 401, 791, doi: 10.1111/j.1365-2966.2009.15715.x

Tran, Q. D., Lutz, D., Genzel, R., et al. 2001, ApJ, 552, 527, doi: 10.1086/320543

Voit, G. M. 1992, MNRAS, 258, 841, doi: 10.1093/mnras/258.4.841
Weinberger, R., Springel, V., & Pakmor, R. 2020, ApJS, 248, 32, doi: 10.3847/1538-4365/ab908c
Xie, Y., & Ho, L. C. 2022, ApJ, 925, 218, doi: 10.3847/1538-4357/ac32e2
Xie, Y., Ho, L. C., Li, A., & Shangguan, J. 2018, ApJ, 860, 154, doi: 10.3847/1538-4357/aac3dc